Journal of Mining and Environment (JME), Vol. 14, No. 2, 2023, 601-618

Shahrood University of Technology

Journal of Mining and Environment (JME)

Journal homepage: www.jme.shahroodut.ac.ir

Iranian Society of Mining Engineering (IRSME)

Analytical Solutions of First-order Displacement Discontinuity Elements in Poroelasticity

Mohammad Hosein Dehghani Firoozabadi[1], Mohammad Fatehi Marji[1], Abolfazl Abdollahipour[2]*, Alireza Yarahmadi Bafghi[1], and Yousef Mirzaeian[1]

1. Department of Mining and Metallurgical Engineering, Faculty of Engineering, Yazd University, Yazd, Iran
2. School of Mining Engineering, College of Engineering, University of Tehran, Tehran, Iran

Article Info

Received 7 February 2023

Received in Revised form 28 April 2023

Accepted 16 May 2023

Published online 16 May 2023

DOI:10.22044/jme.2023.12631.2296

Keywords

Displacement Discontinuity Method

First-order Elements

Poroelastic, Pore Pressure

Fundamental Solutions

Influence Functions

Abstract

The presence of pores and cracks in porous and fractured rocks is mostly accompanied by fluid flow. Poroelasticity can be used for the accurate modeling of many rock structures in the petroleum industry. The approach of the stress to the value of the fracture stress and the effect of pore pressure on the deformation of rock are among the effects of fluid on the mechanical behavior of the medium. Due to the deformation-diffusion property of porous media, governing equations, strain-displacement, and stress-strain relationships can be changed to each other. In this study, constitutive equations and relationships necessary to investigate the behavior and reaction of rock in a porous environment are stated. Independent and time-dependent differential equations for an impulse and point fluid source are used to obtain the fundamental solutions. Influence functions are obtained by using the shape functions in the formulation of the fundamental solutions and integrating them. To check the validity and correctness of provided formulation, several examples are mentioned. In the first two examples, numerical application and analytical solution are used at different times and in undrained and drained conditions. In times 0 (undrained response of medium) and 4500 seconds (drained response of medium), there is good coordination and agreement between the numerical and analytical results. In the third example, using the numerical application, a crack propagation path in the wellbore wall is obtained, which is naturally in the direction of maximum horizontal stress.

1. Introduction

The boundary element method (BEM) is divided into two parts, indirect and direct [1]. In the indirect method, the solution is first executed for the singularities that satisfy the specified boundary conditions. The unknown parameters are then provided indirectly through the standard numerical techniques in terms of these singular solutions. The direct method can directly provide the unknown boundary parameters (stresses and displacements) based on the specified boundary conditions. In boundary element-based methods, since the governing differential equations are solved exactly in the domain of the problem, they result in high accuracy in the solutions. The BEM performs discretization at the boundaries, thus decreasing the dimensionality of the problem. This leads to a smaller system of equations that are very cost-effective, as it significantly decreases the information required for analysis.

The Displacement Discontinuity Method (DDM) is an indirect boundary element method that is utilized for solving linear elastic fracture mechanics (LFEM) problems. The method was first introduced by Crouch and Starfield [2, 3]. In this method, stresses and displacements at a point are provided according to the normal and shear displacement discontinuities. Many studies illustrated how to use constant ordinary elements in DDM [4-6]. The main advantage of using these elements is their simplicity; however, they cannot correctly forecast the stresses and displacements in the field points adjacent to the boundaries. Moreover, the singularity changes $1/r^{0.5}$ and $r^{0.5}$ in

Corresponding author: Abdollahipour@ut.ac.ir (A. Abdollahipour)

the stresses and displacement equations, causing the calculation precision at the neighborhood of the crack tip to severely diminish [7]. In this regard, first-order [8, 9], second-order [10, 11], and third-order [12, 13] elements have been utilized to conquer these problems and obtain more correct values of stresses and displacements along boundaries. Based on the strain elasticity stretching notion, Exadaktylos *et al*. also presented a new constant displacement discontinuity element formulation. This new method substantially makes better the accuracy of DDM without using higher-order and crack-tip elements [14-16]. However, this formulation does not handle the crack tip singularities. Therefore, crack tip elements were presented to remove the obstacle [17]. To significantly improve the accuracy of analysis in crack problems, ordinary and crack tip higher-order elements are used simultaneously. Yan *et al*. have presented constant crack tip elements to utilize in the DDM [18]; they developed the method of fatigue crack growth in structures having multiple cracks [19]. Li *et al*. have utilized a method composed of the constant element displacement discontinuity method and meshless procedures to amplify the crack in the static and cyclic loading conditions [20]. Discontinuities are the main flow channels in sub-surface rocks. Change in the fluid pressure causes matrix deformation and stress change; matrix deformation, in turn, causes fluid volume change and fluid pressure change. Possible fracture propagation leads to changes in pore pressure and stress in the whole field. Variations in pore pressure and stress at any point affect the fracture and induce fracture deformation. This makes media exhibit a strong coupling of mechanical and hydraulic behavior. To investigate this coupled hydro-mechanical behavior, the poroelasticity theory has been developed. Problems such as hydraulic fracturing [21-25], in-situ stress measurement [26-28], and geothermal [29-32] take place in sub-surface rocks that are mostly filled with discontinuities (such as faults) and pores. These discontinuities and pores can be saturated with water, oil, etc. These fluids can affect the stress (i.e. effective stresses due to the pore pressure effect) and displacement fields in rocks. Also pore fluid flow happens due to the pore pressure gradient in the rock. The flow can also be in response to variations in macroscopic stresses caused by natural factors [33]. In order to accurately model these coupled internal reactions, all of these couplings must be involved. The DDM has been coupled with other methods such as the FDM and the FEM to investigate the poroelastic effects of fracture [34-36]. For instance, Ji used the DDM to simulate discontinuity-propagation in porous media and coupled it with the FDM to simulate the fluid response. Yin *et al*. coupled the DDM and the FEM to study poroelastic effects in reservoirs. Bobet and Yu presented a closed-form solution of the crack-tip stress field [37]. They illustrated that the induced stresses during the draining of the media were higher than the stresses around the crack tip under pressure in a saturated media. Recently, many studies have focused on presenting a mathematical formulation or analytical solution for the hydraulic fracture problem in a porous rock [38-46]. Yaylacı *et al*. have used finite element and artificial intelligence to study contact problem and functionally graded materials [1–4].

The development of a new poroelastic numerical method is a significant contribution to the field of geomechanics, and has numerous applications in both academia and industry. This new method is unique compared to other numerical studies because it incorporates the effects of fluid flow and deformation of porous media in a single framework. The method can accurately capture the complex interactions between the fluid and solid phases of porous media, which is crucial for predicting the behavior of underground structures and oil reservoirs. Additionally, the new method allows for the simulation of both undrained and drained conditions, which is not commonly available in other numerical methods. This new method can be used to predict the deformation, stress, and fluid flow behavior of underground structures such as tunnels and dams, as well as the hydrocarbon extraction behavior in oil reservoirs. The originality of this method lies in its ability to provide accurate results for a wide range of applications in geomechanics and petroleum engineering, making it a valuable tool for researchers and practitioners in the field. In this study, governing equations of a porous medium are presented. Then the required fundamental solutions for the poroelastic first-order DDM are derived. After that, influence functions of first-order DDM in a poroelastic rock are introduced. Finally, validation of the new formulation is shown by citing two examples.

2. Illustration of First-order Displacement Discontinuity

A displacement discontinuity element of length $2a$ along the x-axis is illustrated in Figure 1(a), which is characterized by a total displacement discontinuity distribution $u(ʒ)$. Considering u_x and u_y components of the total displacement discontinuity $u(ʒ)$ to be constant and equal to D_x and D_y, respectively, in the interval ($-a$, $+a$) as illustrated in Figure 1(b), two displacement discontinuity element surfaces can be noted, one on the negative side of y and another one on the positive side y.

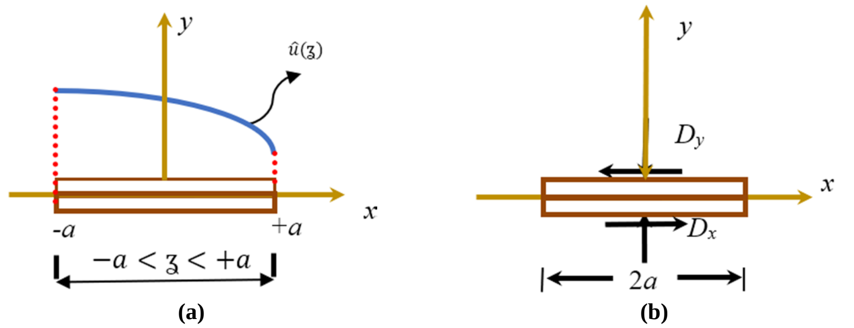

Figure 1. a) Distribution of u(ʒ) for totaldisplacement discontinuity element. b) Components of the constant element.

The displacement includes a constant change in value when crossing from one side of the displacement discontinuity element to the other side, which may be defined as:

$$\begin{cases} Dx = ux(x,0-) - ux(x,0+) \\ Dy = uy(x,0-) - uy(x,0+) \end{cases} \quad (1)$$

The positive sign convention of D_x and D_y is illustrated in Figure 1(b) and depicts that when the two surfaces of the displacement discontinuity overlap, D_y is positive, which causes a physically impossible situation. This conceptual difficulty is resolved by considering that the element has a finite thickness in its undeformed state, which is small evaluated to its length but bigger than D_y [3].

The first-order element displacement discontinuity formulation is based on the analytical integration of first-order shape functions of straight-line displacement discontinuity elements.

Figure 2 (a) illustrates the linear displacement discontinuity distribution, which may be expressed in a total form as:

$$D_i(ʒ)=N_1(ʒ)(D_i)_1+N_2(ʒ)(D_i)_2 \quad i=x,y \quad (2)$$

where $(D_i)_1$ and $(D_i)_2$ is the first-order displacement discontinuities, and

$$\begin{cases} N1(ʒ) = -(ʒ - a2)/(a1 + a2) \\ N2(ʒ) = (ʒ - a1)/(a1 + a2) \end{cases} \quad (3)$$

are their first-order collocation shape functions. It should be considered that a first-order element has 2 nodes, which are the centers of the two elements within the path element [47].

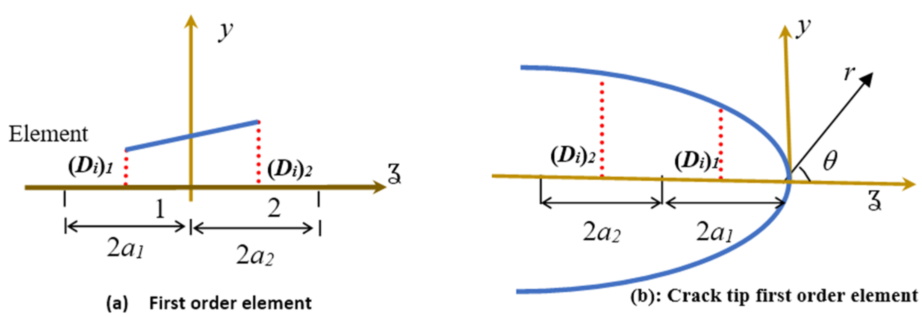

Figure 2. Location of nodes for first-order displacement discontinuity elements.

3. Characteristics of porous media

The notion of first-order, isotropic poroelasticity was explained by Biot for modeling the reply of fluid-saturated porous solids [48] and was developed by other [49, 50]. According to the basic formula of Biot, the basic dynamic parameters of total stress σ_{ij} and pore pressure p along with their corresponding quantities, solid strain $e_{ij} = (u_{i,j} + u_{j,i})/2$ and variation of fluid volume per unit reference ʒ are considered here. A fixed set of parameters for the first order isotropic notion is shear modulus G, drained and undrained Poisson ratios, which are, respectively, $\nu = (3K - 2G)/2\ (3K + G)$, $\nu_u = (3Ku - 2G)/2\ (3Ku + G)$(drained and undrained bulk moduli K and Ku), Skempton's pore pressure coefficient S (ratio of induced pore pressure to change of confined pressure in undrained conditions), and permeability coefficient $\kappa = k/\mu$ (where k is intrinsic permeability and μ fluid dynamic viscosity) [48]. The governing equations of the first-order isotropic poroelasticity consist of the following [48]:

- Constitutive equations:

$$\sigma_{ij} = 2Ge_{ij} + \frac{2G\nu}{1-2\nu}\delta_{ij}e - \alpha\delta_{ij}p \tag{4}$$

$$p = -\frac{2GS(1+\nu_u)}{3(1-2\nu_u)}e + \frac{2GS^2(1-2\nu)(1+\nu_u)^2}{9(\nu_u-\nu)(1-2\nu_u)}\mathfrak{z} \tag{5}$$

- Equilibrium equations:

$$\sigma_{ij,j} = -F_i \tag{6}$$

- Darcy's law

$$q_i = -\kappa\left(p_{,i} - f_i\right) \tag{7}$$

- Continuity equation:

$$\frac{\partial\mathfrak{z}}{\partial t} + q_{i,i} = \gamma \tag{8}$$

where in the above equations, $e = e_{ii}$ is the volumetric strain, $Fi = \rho g_i$ bulk body force (solid and fluid), g_i gravity component in i direction, n porosity, q_i specific discharge, $\mathfrak{z}$change of fluid content, $\rho = (1-n)\rho_s + \phi\rho_f$ bulk density, ρ_s and ρ_f solid and fluid part densities, respectively, $f_i = \rho_f g_i$ fluid body force, γ fluid injection rate from the fluid source, and α is the Biot coefficient of effective stress, defined as:

$$\alpha = \frac{3(\nu_u-\nu)}{S(1-2\nu)(1+\nu_u)} \tag{9}$$

The above can be combined to yield a set of field equations in terms of displacement and fluid content variation. Combining Equations (4) to (6) yields an elasticity equation with a fluid coupling term:

$$G\nabla^2u_i + \frac{G}{1-2\nu_u}e_{,i} - \frac{2GS(1+\nu_u)}{3(1-2\nu_u)}\mathfrak{z}_{,i} = -F_i \tag{10}$$

Combining Equations (5), (7), and (8), and also using Equation (10) create the following diffusion equation:

$$\frac{\partial\mathfrak{z}}{\partial t} - c\nabla^2\mathfrak{z} = \frac{kS(1+\nu_u)}{3(1-\nu_u)}F_{i,i} - kf_{i,i} + \gamma \tag{11}$$

where:

$$C = \frac{2kS^2G(1-\nu)(1+\nu_u)^2}{9(1-\nu_u)(\nu_u-\nu)} \tag{12}$$

is a consolidation coefficient [50].The above equations can be utilized to obtain the needed solution for the first-order DDM in porous rock.

4. Influence Functions of First-order Displacement Discontinuity Method in a Poroelastic Medium

Appendix A presents the poroelastic solution of point plane strain displacement discontinuity [55, 56]. Poroelastic influence functions for the first order can be obtained by distributing and integrating this solution over an element domain ς^{λ} located on the local s-axis (Figure 3). For example, utilizing the following integrals, it is possible to present the value of the stress in the local s direction caused by the shear displacement discontinuity.

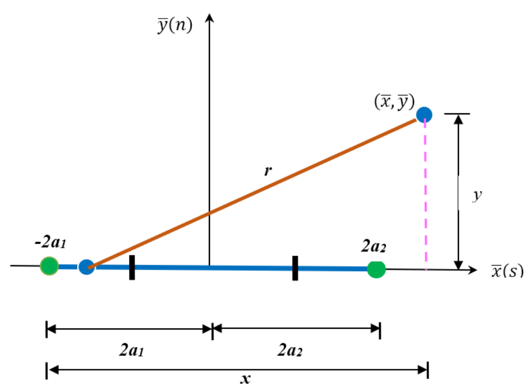

Figure 3. A first-order element in local coordinates.

where: $(D_n)_1N_1(\mathfrak{z})\sigma_{211}$, $(D_n)_2N_2(\mathfrak{z})\sigma_{211}$, $(D_n)_1N_1(\mathfrak{z})\odot(\sigma_{211})$, and $(D_n)_2N_2(\mathfrak{z})\odot(\sigma_{211})$ in these equations are the fundamental solutions, which are defined in Equations (A1) and (A2) of Appendix A and $I = 2$, $j = k = 1$. For the time-independent and time-dependent influence functions, considering Equations (13) and (14) the complete set of integrals and their solutions is provided in Appendix B.

$$\sigma_{yx}^{ds} = \int_{-2a_1}^{+2a_1}(D_s)_1 N_1(\mathfrak{z})\sigma_{211}d\mathfrak{z} + \int_{-2a_2}^{+2a_2}(D_s)_2 N_2(\mathfrak{z})\sigma_{211}d\mathfrak{z} =$$

$$\begin{aligned}
&\frac{G}{2\pi(1-\nu_u)}\left[\frac{-1}{a}\int_{-2a_1}^{+2a_1}\left[\frac{8(x-\mathfrak{z})y^4}{((x-\mathfrak{z})^2+y^2)^3}-\frac{4(x-\mathfrak{z})y^2}{((x-\mathfrak{z})^2+y^2)^2}-\frac{(x-\mathfrak{z})}{((x-\mathfrak{z})^2+y^2)}\right]d\mathfrak{z}\right.\\
&\quad+\frac{1}{2}\int_{-2a_1}^{+2a_1}\left[\frac{8y^4}{((x-\mathfrak{z})^2+y^2)^3}-\frac{4y^2}{((x-\mathfrak{z})^2+y^2)^2}-\frac{1}{((x-\mathfrak{z})^2+y^2)}\right]d\mathfrak{z}\\
&\quad+\frac{1}{a}\int_{-2a_2}^{+2a_2}\left[\frac{8(x-\mathfrak{z})y^4}{((x-\mathfrak{z})^2+y^2)^3}-\frac{4(x-\mathfrak{z})y^2}{((x-\mathfrak{z})^2+y^2)^2}-\frac{(x-\mathfrak{z})}{((x-\mathfrak{z})^2+y^2)}\right]d\mathfrak{z}\\
&\quad\left.+\frac{1}{2}\int_{-2a_2}^{+2a_2}\left[\frac{8y^4}{((x-\mathfrak{z})^2+y^2)^3}-\frac{4y^2}{((x-\mathfrak{z})^2+y^2)^2}-\frac{1}{((x-\mathfrak{z})^2+y^2)}\right]d\mathfrak{z}\right]\\
&\quad=-\frac{G}{4\pi(1-\nu_u)}\left[\left(\frac{(x-\mathfrak{z})((x-\mathfrak{z})^2+3y^2)}{((x-\mathfrak{z})^2+y^2)^2}\right)\Bigg|_{\mathfrak{z}=-2a_1}^{\mathfrak{z}=+2a_1}+\left(\frac{(x-\mathfrak{z})((x-\mathfrak{z})^2+3y^2)}{((x-\mathfrak{z})^2+y^2)^2}\right)\Bigg|_{\mathfrak{z}=-2a_2}^{\mathfrak{z}=+2a_2}\right]\\
&\quad=-\frac{G}{4\pi(1-\nu_u)}\left[\left(\frac{(x-2a_1)((x-2a_1)^2+3y^2)}{((x-2a_1)^2+y^2)^2}-\frac{(x+2a_1)((x+2a_1)^2+3y^2)}{((x+2a_1)^2+y^2)^2}\right)\right.\\
&\quad\left.+\left(\frac{(x-2a_2)((x-2a_2)^2+3y^2)}{((x-2a_2)^2+y^2)^2}-\frac{(x+2a_2)((x+2a_2)^2+3y^2)}{((x+2a_2)^2+y^2)^2}\right)\right]
\end{aligned} \tag{13}$$

$$\odot\sigma_{yx}^{ds} = \int_{-2a_1}^{+2a_1}(D_s)_1 N_1(\mathfrak{z})\odot(\sigma_{211})d\mathfrak{z} + \int_{-2a_2}^{+2a_2}(D_s)_2 N_2(\mathfrak{z})\odot(\sigma_{211})d\mathfrak{z} =$$

$$\begin{aligned}
&\frac{2Gc(\nu_u-\nu)}{\pi(1-\nu_u)(1-\nu)}\left[\frac{-1}{a}\frac{1}{((x-\mathfrak{z})^2+y^2)^3}\times\left[(x-\mathfrak{z})^2(3y^2-(x-\mathfrak{z})^3)\left[1-(1+\xi^2)e^{-\xi^2}\right]+2(x-\mathfrak{z})^4\xi^4e^{-\xi^2}\right]\Big|_{\mathfrak{z}=-2a_1}^{\mathfrak{z}=+2a_1}\right.\\
&\quad+\frac{1}{2}\frac{1}{((x-\mathfrak{z})^2+y^2)^3}\times\left[(x-\mathfrak{z})(3y^2-(x-\mathfrak{z})^2)\left[1-(1+\xi^2)e^{-\xi^2}\right]+2(x-\mathfrak{z})^3\xi^4e^{-\xi^2}\right]\Big|_{\mathfrak{z}=-2a_1}^{\mathfrak{z}=+2a_1}\\
&\quad+\frac{1}{a}\frac{1}{((x-\mathfrak{z})^2+y^2)^3}\times\left[(x-\mathfrak{z})^2(3y^2-(x-\mathfrak{z})^3)\left[1-(1+\xi^2)e^{-\xi^2}\right]+2(x-\mathfrak{z})^4\xi^4e^{-\xi^2}\right]\Big|_{\mathfrak{z}=-2a_2}^{\mathfrak{z}=+2a_2}\\
&\quad\left.+\frac{1}{2}\frac{1}{((x-\mathfrak{z})^2+y^2)^3}\times\left[(x-\mathfrak{z})(3y^2-(x-\mathfrak{z})^2)\left[1-(1+\xi^2)e^{-\xi^2}\right]+2(x-\mathfrak{z})^3\xi^4e^{-\xi^2}\right]\Big|_{\mathfrak{z}=-2a_2}^{\mathfrak{z}=+2a_2}\right]\\
&\quad=\frac{Gc(\nu_u-\nu)}{\pi(1-\nu_u)(1-\nu)}\left[\left(\frac{1}{((x-2a_1)^2+y^2)^3}-\frac{1}{((x+2a_1)^2+y^2)^3}\right)\right.\\
&\quad\times\left(\left[(x-2a_1)(3y^2-(x-2a_1)^2)\left[1-(1+\xi^2)e^{-\xi^2}\right]+2(x-2a_1)^3\xi^4e^{-\xi^2}\right]\right.\\
&\quad\left.-\left[(x+2a_1)(3y^2-(x+2a_1)^2)\left[1-(1+\xi^2)e^{-\xi^2}\right]+2(x+2a_1)^3\xi^4e^{-\xi^2}\right]\right)\\
&\quad+\left(\frac{1}{((x-2a_2)^2+y^2)^3}-\frac{1}{((x+2a_2)^2+y^2)^3}\right)\\
&\quad\times\left(\left[(x-2a_2)(3y^2-(x-2a_2)^2)\left[1-(1+\xi^2)e^{-\xi^2}\right]+2(x-2a_2)^3\xi^4e^{-\xi^2}\right]\right.\\
&\quad\left.\left.-\left[(x+2a_2)(3y^2-(x+2a_2)^2)\left[1-(1+\xi^2)e^{-\xi^2}\right]+2(x+2a_2)^3\xi^4e^{-\xi^2}\right]\right)\right]
\end{aligned} \tag{14}$$

5. Validation of the Proposed Formulation

In the following, several examples of crack opening displacement (COD) and crack propagation are presented to investigate the performance and accuracy of the provided formulation. The first two examples show the crack opening displacement using analytical and numerical methods and compare the results. The third example shows the crack propagation path in the wellbore wall using the written code [58].

5.1. Crack opening displacement in undrained and drained conditions

In this section, a combination of analytical and numerical examples is presented to validate provided formulation. Crack opening displacement (COD) is evaluated in these examples. Snowden's solution is used in the analytical part. The exact value of *COD* in Equation (15) can be computed [57].

$$COD = \sqrt{L^2 - x^2}\,\frac{2I(1-\nu)}{G} \tag{15}$$

where I, ν, G, and L are the internal pressure, poisson coefficient, shear modulus, and crack length, respectively, and $-L \leq x \leq +L$.

Figure 4 shows a thin crack with constant internal pressure I and length 2L.

In the numerical part, the code written for poroelastic media [54] is used, because the calculation of influence functions is the last step before numerical implementation. Therefore, the correctness of the prepared formulation results in providing a correct output of the numerical method. The following examples include two sections with undrained conditions and drained conditions.

5.1.1. Crack opening displacement in undrained condition

In general, the undrained response of the medium expresses the condition that the time required for fluid movement between rock elements by mass transfer is very short so that no mass transfer takes place.

Among parameters that allow a better understanding of behavior from a poroelastic medium are Biot's coefficient and Skempton's coefficient.

To check the correctness of the prepared formulation, crack opening displacement in poroelastic media is investigated. In this example, modeled crack length is one meter (the crack is horizontal and without an angle). The number of elements forming the crack is 20. The considered parameters for the model are given in Table 1.

Numerical and analytical predictions of crack opening displacement are compared in Figure 5. As can be seen, analytical and numerical charts are in good agreement with each other. The error in estimating crack opening displacement for the first-order element mode is 1.15% lower than of constant element mode.

5.1.2. Crack opening displacement in drained condition

In general, a drained response occurs after a relatively long time, and shows a state in that fluid is not stationary in pores. As a result, deformation changes from a short time to a long time.

The number of elements, length, and crack mode are the same as in the previous example.

The considered parameters for the model are given in Table 2.

Numerical and analytical predictions of crack opening displacement are compared in Figure 6. As can be seen, analytical and numerical charts are in good agreement with each other. The error in estimating crack opening displacement for the first-order element mode is 0.52% lower than for the constant element mode.

Table 1. Parameters used in model analysis.

Undrained Poisson ratio (νu)	0.29
Skempton's coefficient (S)	0.90
Permeability (κ) (mdarcy)	1
Biot's coefficient (α)	0.67
Generalized consolidation coefficient (c) (m2/s)	0.003
Shear modulus(G) (GPa)	13
Internal pressure (MPa)	25
Time (s)	0

Table 2. Parameters used in model analysis.

Drained poisson ratio (ν)	0.1
Skempton's coefficient (S)	0.90
Permeability (κ) (mdarcy)	1
Biot's coefficient (α)	0.67
Generalized consolidation coefficient (c) (m2/s)	0.003
Shear modulus (G) (GPa)	13
Internal pressure (MPa)	25
Length of each time step (s)	0.05
Time (s)	4500

5.2. Effect of angle of initial cracks relative to in-situ stresses on crack propagation process in well wall

The effect of the angle of the initial cracks on the crack propagation path is investigated under different insitu stresses. Figure 7 shows the overview of modeling. The considered parameters for the model are given in Tables 2 and 3. Naturally, the path of crack propagation should be in the direction of maximum horizontal stress (σ_H), which is obtained in the three cases of Figure 8.

Table 3. Parameters used in model analysis.

α for the chart (a) (degree)	0
I/σ_H for the chart (a)	1.2
σ_h/σ_H for the chart (a)	0.5
α for chart (b) (degree)	30
I/σ_H for chart (b)	1.5
σ_h/σ_H for chart (b)	0.6
α for chart (c) (degree)	60
I/σ_H for chart (c)	1.0
σ_h/σ_H for chart (c)	0.5
R (radius of the wellbore) (meter)	0.5
an (initial crack length) (meter)	1.0

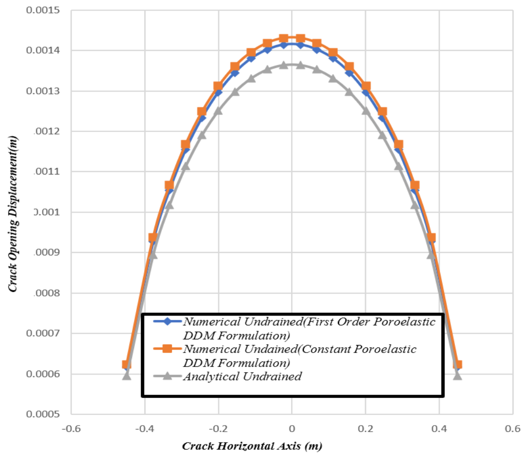

Figure 5. Comparison of analytical and numerical (first-order poroelastic DDM formulation and constant poroelastic DDM formulation) results of *COD* in undrained conditions.

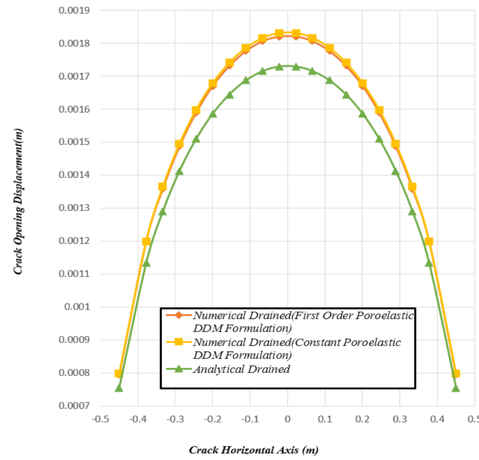

Figure 6. Comparison analytical and numerical (first-order poroelastic DDM formulation and constant poroelastic DDM formulation) results of *COD* in drained condition.

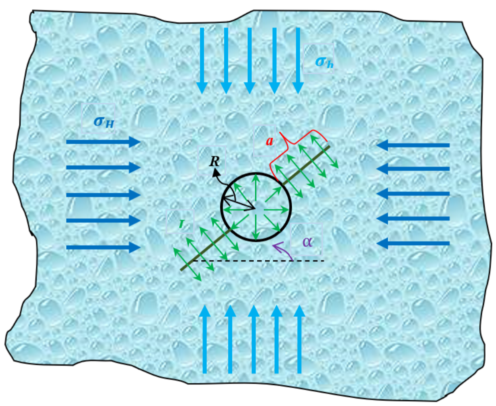

Figure 7. An overview of the modeling of the effect of the angle of initial cracks along with in situ stresses on the crack propagation process in the well wall.

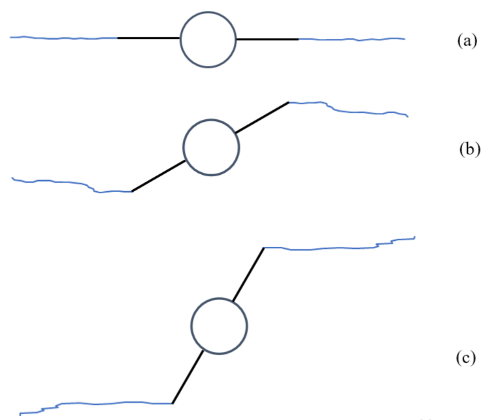

Figure 8. Crack propagation path at different angles and in-situ stresses in well wall.

6. Conclusions

Fundamental solutions in the displacement discontinuity method (*DDM*) contribute a displacement jump since this method is suitable for problems including fractures and discontinuities. However, the basic *DDM* and its higher-order extensions are all confined to elastic problems. In geo-mechanics, many situations such as hydraulic fracturing, in-situ stress measurement, and geothermal take place in a poroelastic media.

Because the porous media are affected by the deformation-diffusion reaction, it is necessary to utilize the theory of poroelasticity. The possibility of developing boundary element methods for porous media may be achieved when the fundamental solutions of poroelastic media are given. In order to derive the fundamental solutions for the porous first-order displacement discontinuity, the fundamental solutions of the first-order displacement discontinuity of the impulse point and the source were utilized. The fundamental solution makes the influence function in the final *DDM* formulation. First, the fundamental solutions were derived. Then the first-order shape functions were calculated. Finally, the shape functions of the fundamental solutions were integrated to calculate the influence functions. The validity of the new formulation was proved using the numerical application and analytical solutions. The results of numerical models were obtained at 0 and 4500 seconds. The results of analytical models obtained utilizing the undrained and drained Poisson's ratio. These results, which are stated by citing two examples, show a good agreement and coordination between the numerical and analytical results. In the end, by mentioning another example, the path of crack propagation in the well wall is demonstrated using the numerical application, which is consistent with the natural results.

References

[1]. Crouch, SL. and Starfield, AM. (1983). Boundary Element Methods in Solid Mechanics: With Applications in Rock Mechanics and Geological Engineering. Allen & Unwin.

[2]. Crouch, SL. (1976). Engineering U of MD of C and M, Program NSF (U.S). RA to NN. Analysis of Stresses and Displacements Around Underground Excavations.

[3]. Crouch, SL. (1976). Solution of plane elasticity problems by the displacement discontinuity method. I. Infinite body solution. Int J Numer Methods Eng. 10 (2): 301–343.

[4]. Chaoxi, L. and Suaris, W. (1991). Hadamard's principle for displacement discontinuity modeling of cracks. Eng FractMech; 39:141–5.

[5]. Fatehi-Marji, M. (2011). On the crack propagation mechanism of brittle rocks under various loading conditions.

[6]. Haeri, H. Shahriar, K. Fatehi-Marji, M. and Moarefvand, P. (2014). Experimental and numerical study of crack propagation and coalescence in pre-cracked rock-like disks. Int J Rock Mech Min Sci; 67:20–8.

[7]. Fatehi-Marji, M. (2014). Rock fracture mechanics with displacement discontinuity method. Ger L Lambert Acad Publ.

[8]. Crawford, A.M. and Curran, J.H. (1982). Higher-order functional variation displacement discontinuity elements. Int J Rock Mech Min Sci Geomech Abstr ;19: 143–8.

[9]. Napier, J.A.L. and Malan, D.F. (1997). A viscoplastic discontinuum model of time-dependent fracture and seismicity effects in brittle rock. Int J Rock Mech Min Sci; 34 (7): 1075–89.

[10]. Fatehi-Marji, M. (2015). Simulation of crack coalescence mechanism underneath single and double disc cutters by higher order displacement discontinuity method. J Cent South Univ; 22 (3):1045–54.

[11]. Abdollahipour, A. and Fatehi-Marji, M. (2020). A thermo-hydromechanical displacement discontinuity method to model fractures in high-pressure, high-temperature environments. RenewEnergy.

[12]. Fatehi-Marji, M. (1996). Modeling of cracks in rock fragmentation with a higher order displacement discontinuity method. Ankara, Turkey: Middle East Technical University.

[13]. Abdollahipour, A. Fatehi-Marji, M. Yarahmadi-Bafghi, A. and Gholamnejad, J. (2016). On the accuracy of higher order displacement discontinuity method (HODDM) in the solution of linear elastic fracture mechanics problems. J Cent South Univ; 23 (11):2941–50.

[14]. Exadaktylos, G. and Xiroudakis, G. (2010). The G2 constant displacement discontinuity method–Part I: Solution of plane crack problems. Int J Solids Struct; 47(18-19): 2568–77.

[15]. Dehghani-Firoozabadi, M.H. Fatehi-Marji, M. Abdollahipour, A. Yarahamdi-Bafghi, A. and Mirzaeian, Y. (2022). Simulation of Crack Propagation Mechanism in Porous Media using Modified linear Element Displacement Discontinuity Method. Volume 13, Issue 3, July 2022, Pages 903-927.

[16]. Exadaktylos, G. and Xiroudakis G. (2010). A G2 constant displacement discontinuity element for analysis of crack problems. Comput Mech; 45 (4):245–61.

[17]. Fatehi-Marji, M. Hosseini-Nasab, H. and Kohsary, A.H. (2007). A new cubic element formulation of the displacement discontinuity method using three special crack tip elements for crack analysis. JP J Solids Struct; 1:61–91.

[18]. Yan, X. (2005). An efficient and accurate numerical method of stress intensity factors calculation of a branched crack. J Appl Mech; 72:330–40.

[19]. Yan, X. (2006). Multiple crack fatigue growth modeling by displacement discontinuity method with crack-tip elements. Appl Math Model; 30 (6):489–508.

[20]. Li, J. Sladek, J. Sladek, V. and Wen, P.H. (2020). Hybrid meshless displacement discontinuity method (MDDM) in fracture mechanics: static and dynamic. Eur J Mech

[21]. Naredran, V.M. and Cleary, M.P. (1983). Analysis of growth and interaction of multiple hydraulic fractures. Reserv. Stimul. Symp., San Francisco.

[22]. Adachi, J.I. and Detournay, E. (2008). Plane strain propagation of a hydraulic fracture in a permeable rock. Engng Fract Mech 2008; 75:4666–94. mech.04.006.

[23]. Ito, T. (2008). Effect of pore pressure gradient on fracture initiation in fluid saturated porous media: Rock. Eng Fract Mech; 75:1753–62.

[24]. Huang, J. Griffiths, D.V-V and Wong, S. (2012). Initiation pressure, location and orientation of hydraulic fracture. Int J Rock Mech Min Sci; 49: 59–67.2011.11.014.

[25]. Yu, W. Luo, Z. Javadpour, F. Varavei, A. and Sepehrnoori, K. (2014). Sensitivity analysis of hydraulic fracture geometry in shale gas reservoirs. JPetSciEng; 113:1–7.

[26]. Bush, D.D. and Barton, N. (1989). Application of small-scale hydraulic fracturing for stress measurements in bedded salt. Int J Rock Mech Min Sci Geomech Abstr; 26:629–35.

[27]. Schmitt, D.R. and Zoback, M.D. (1989). Poroelastic effects in the determination of the maximum horizontal principal stress in hydraulic fracturing tests—A proposed breakdown equation employing a modified effective stress relation for tensile failure. Int J Rock Mech Min Sci Geomech Abstr; 26:499–506.

[28]. Abdollahipour, A. Fatehi Marji, M. and Yarahmadi-Bafghi, A.R. (2013). A fracture mechanics concept of in-situ stress measurement by hydraulic fracturing test. 6th Int. Symp. In-situ Rock Stress, Sendai, Japan: ISRM.

[29]. Legarth, B. Huenges, E. and Zimmermann, G. (2005). Hydraulic fracturing in a sedimentary geothermal reservoir: Results and implications. Int J Rock Mech Min Sci ;42:1028–1041.

[30]. Reinicke, A. Zimmermann, G. (2010). Hydraulic stimulation of a deep sandstone reservoir to develop an enhanced geothermal system:laboratory and field experiments. Geothermics39:70–77.

[31]. Davis, R. and Carter, L. (2013). Fracking Doesn't Cause Significant Earthquakes. Durham Univesity.

[32]. Hofmann, H. Babadagli, T. and Zimmermann, G. (2014). Hot water generation for oil sands processing from enhanced geothermal systems: Process simulation for different hydraulic fracturing scenarios. Appl Energy 113:524–547.

[33]. Jaeger, J. Cook, N. and Zimmerman, R. (2009). Fundamentals of rock mechanics. Wiley, New York.

[34]. Boonei, T.J. Ingraffea, A.R. Roegiers, J.C. (1991). Simulation of hydraulic fracture propagation in poroelastic rock with application to stress measurement techniques. Int J Rock Mech Min Sci Geomech abstr 28:1–14.

[35]. Yin, S. Dusseault, M.B. and Rothenburg, L. (2007). Analytical and numerical analysis of pressure drawdown in a poroelastic reservoir with complete overburden effect considered. Adv Water Resour 30:1160–1167.

[36]. Ji, L. (2013). Geomechanical aspects of fracture growth in a poroelastic, chemically reactive environment. The University of Texas at Austin.

[37]. Bobet, A. and Yu, H. (2015). Stress field near the tip ofa crack in a poroelastic transversely anisotropic saturated rock. Eng Fract Mech 141:1–18.

[38]. Greetesma, J. and de Klerk, F. (1969). A rapid method of predicting width and extent of hydraulic induced fractures. J Pet Tech 21:1571–1581.

[39]. Detournay, E. (2004). Propagation regimes of fluid-driven fractures in impermeable rocks. Int J Geomech 4:35–45.

[40]. Mitchell, S, Kuske, R. and Peirce, A. (2006). An asymptotic framework for finite hydraulic fractures including leak-off. SIAM J Appl Math 67:364–386

[41]. Garagash, D. (2007). Plane-strain propagation of a fluid-driven fracture during injection and shut-in: asymptotics of large toughness. Engng Fract Mech 74:456–481.

[42]. Mitchell, S. Kuske, R. and Peirce, A. (2007). An asymptotic framework for the analysis of hydraulic fractures: the impermeable case. J Appl Mech Trans ASME 74:365–372.

[43]. Hu, J. and Garagash, D. (2010). Plane-strain propagation of a fluid-driven crack in a permeable rock with fracture toughness. J Eng Mech ASCE 136:1152–1166.

[44]. Lobao, M. Eve, R. Owen, DRJ. *et al*. (2010). Modelling of hydrofracture flow in porous media. EngngComput 27:129–154.

[45]. Behnia, M. Goshtasbi, K. Fatehi Marji, M. and Golshani, A. (2012). On the crack propagation modeling of hydraulic fracturing by a hybridized displacement discontinuity/ boundary collocation method. J Min Environ; 2.

[46]. Darvish, H. Nouri-Taleghani, M. Shokrollahi, A. and Tatar, A. (2015). Geo-mechanical modeling and selection of suitable layer for hydraulic fracturing operation in an oil reservoir (south west of Iran). J African Earth Sci; 111:409–20.

[47]. Yaylaci, M. Merve, A. Ecren, U. Yaylaci H. (2022). The contact problem of the functionally graded layer resting on rigid foundation pressed via rigid punch, Steel and Composite Structures. 43 661–672.

[48]. M. Yaylacı, M. Abanoz, E.U. Yaylacı, H. Ölmez, D.M. Sekban, A. Birinci, Evaluation of the contact problem of functionally graded layer resting on rigid foundation pressed via rigid punch by analytical and numerical (FEM and MLP) methods, Archive of Applied Mechanics. 92 (2022) 1953–1971.

[49]. M. Turan, E. Uzun Yaylacı, M. Yaylacı, Free vibration and buckling of functionally graded porous beams using analytical, finite element, and artificial neural network methods, Archive of Applied Mechanics. 93 (2023) 1351–1372.

[50]. Öner, E. Şengül Şabano, B. Uzun Yaylacı, E. Adıyaman, G. Yaylacı, M. Birinci, A. (2022) On the plane receding contact between two functionally graded layers using computational, finite element and artificial neural network methods, ZAMM - Journal of Applied Mathematics and Mechanics / Zeitschrift Für Angewandte Mathematik Und Mechanik. 102. https://doi.org/10.1002/zamm.202100287.

[51]. Shou, K. J. and Crouch, S. L. (1995). 'A Higher Order Displacement Discontinuity Method for Analysis of Crack Problems'; Int. J. Rock Mech. Min. Sci. and Geomech. Abstr, 32, pp. 49-55.

[52] Biot, MA. (1941). General theory of three-dimensional consolidation. J Appl Phys 12:155–164.

[53]. Verruijt, A. (1969). Elastic storage in aquifers. Flow through porous media. Academic Press, New York, pp 331–376.

[54]. Rice, J.R. and Cleary, M.P. (1976). Some basic stress diffusion solutions for fluid saturated elastic. Rev Geophys 14:227–241.

[55]. Detournay, E. and Cheng, A. (1987). Poroelastic solution of a plane strain point displacement discontinuity.

[56]. Abdollahipour, A. (2015). Crack propagation mechanism in hydraulic fracturing procedure in oil reservoirs. University of Yazd, Yazd.

[57]. Sneddon, I.N. (1951). Fourier transforms. McGraw-Hill Book Company, New York.

Appendix A

$$\sigma_{ijk} = -\frac{G}{2\pi(1-\nu_u)}\delta(t)\frac{1}{r^2}\left[8r_{,i}r_{,j}r_{,k}r_{,2} - 2\left(\delta_{k2}r_{,i}r_{,j} + \delta_{ij}r_{,k}r_{,2}\right) - \left(\delta_{ik}\delta_{j2} + \delta_{jk}\delta_{i2} - \delta_{ij}\delta_{k2}\right)\right] \quad \text{(A.1)}$$

$$\begin{aligned}\odot\sigma_{ijk} = &-\frac{2Gc(v_u - v)}{\pi(1-v)(1-v_u)}\frac{1}{r^4}\Big(\left[24r_{,i}r_{,j}r_{,k}r_{,2} - 12\left(\delta_{ij}r_{,k}r_{,2} + \delta_{k2}r_{,i}r_{,j}\right)\right.\\ &\left.-3\left(\delta_{ik}\delta_{j2} + \delta_{jk}\delta_{i2} - 3\delta_{ij}\delta_{k2}\right)\right]\left[1 - (1+\xi^2)e^{-\xi^2}\right]\\ &-\left[12r_{,i}r_{,j}r_{,k}r_{,2} - 6\left(\delta_{k2}r_{,i}r_{,j} + \delta_{ij}r_{,k}r_{,2}\right) - 2\delta_{ik}\delta_{j2} - 2\delta_{jk}\delta_{i2} + 4\delta_{ij}\delta_{k2}\right]\xi^4 e^{-\xi^2}\\ &-\left[4r_{,i}r_{,j}r_{,k}r_{,2} - 4\left(\delta_{ij}r_{,k}r_{,2} + \delta_{k2}r_{,i}r_{,j}\right) + 4\delta_{ij}\delta_{k2}\right]\xi^6 e^{-\xi^2}\Big)\end{aligned} \quad \text{(A.2)}$$

$$p_i = \frac{SG(1+v_u)}{3\pi(1-v_u)}\delta(t)\frac{1}{r^2}\left(\delta_{i2} - 2r_{,i}r_{,2}\right) \quad \text{(A.3)}$$

$$\odot p_i = \frac{4SGc(1+v_u)}{3\pi(1-v_u)}\frac{1}{r^4}\left(\delta_{i2}\xi^4 e^{-\xi^2} + 2\left(r_{,i}r_{,2} - \mathrm{c}\delta_{i2}\right)\xi^6 e^{-\xi^2}\right) \quad \text{(A.4)}$$

$$q_{ij} = \frac{3c(\nu_u - \nu)}{\pi S(1-\nu)(1+\nu_u)}\delta(t)\frac{1}{r^3}\left(\delta_{i2}r_{,j} + \delta_{j2}r_{,i} + \delta_{ij}r_{,2} - 4r_{,i}r_{,j}r_{,2}\right) \quad \text{(A.5)}$$

$$\odot q_{ij} = -\frac{6c^2(v_u - v)}{\pi S(1-v)(1+v_u)}\frac{1}{r^5}\left[2\left(\delta_{i2}r_{,j} + \delta_{ij}r_{,2} - 3\delta_{j2}r_{,i}\right)\xi^6 e^{-\xi^2} + 4\left(\delta_{j2}r_{,i} - r_{,i}r_{,j}r_{,2}\right)\xi^8 e^{-\xi^2}\right] \quad \text{(A.6)}$$

Appendix B

Time-independent part of influence functions

$$\begin{aligned}\sigma_{yy}^{ds,\lambda} &= (D_s)_1\int_{-2a_1}^{+2a_1} N_1(x-z)\sigma_{221}(x-z,y)\,dz + (D_s)_2\int_{-2a_2}^{+2a_2} N_2(x-z)\sigma_{221}(x-z,y)\,dz =\\ &\frac{G}{2\pi(1-v_u)}\left[\frac{-1}{a}\int_{-2a_1}^{+2a_1}\left[\frac{8(x-z)^2y^3}{((x-z)^2+y^2)^3} - \frac{2y(x-z)^2}{((x-z)^2+y^2)^2}\right]dz + \frac{1}{2}\int_{-2a_1}^{+2a_1}\left[\frac{8(x-z)y^3}{((x-z)^2+y^2)^3} - \frac{2y(x-z)}{((x-z)^2+y^2)^2}\right]dz\right.\\ &\quad+\frac{1}{a}\int_{-2a_2}^{+2a_2}\left[\frac{8(x-z)^2y^3}{((x-z)^2+y^2)^3} - \frac{2y(x-z)^2}{((x-z)^2+y^2)^2}\right]dz\\ &\quad\left.+\frac{1}{2}\int_{-2a_2}^{+2a_2}\left[\frac{8(x-z)y^3}{((x-z)^2+y^2)^3} - \frac{2y(x-z)}{((x-z)^2+y^2)^2}\right]dz\right] =\\ &\frac{G}{4\pi(1-v_u)}\left[\left(\frac{y(y^2-(x-z)^2)}{((x-z)^2+y^2)^2}\right)\Bigg|_{z=-2a_1}^{z=+2a_1} + \left(\frac{y(y^2-(x-z)^2)}{((x-z)^2+y^2)^2}\right)\Bigg|_{z=-2a_2}^{z=+2a_2}\right] =\\ &\frac{G}{4\pi(1-v_u)}\left[\left(\frac{y(y^2-(x-2a_1)^2)}{((x-2a_1)^2+y^2)^2} - \frac{y(y^2-(x+2a_1)^2)}{((x+2a_1)^2+y^2)^2}\right) + \left(\frac{y(y^2-(x-2a_2)^2)}{((x-2a_2)^2+y^2)^2} - \frac{y(y^2-(x+2a_2)^2)}{((x+2a_2)^2+y^2)^2}\right)\right]\end{aligned} \quad \text{(B.1)}$$

$$\sigma_{xx}^{ds,\lambda} = (D_s)_1\int_{-2a_1}^{+2a_1} N_1(x-z)\sigma_{111}(x-z,y)\,dz + (D_s)_2\int_{-2a_2}^{+2a_2} N_2(x-z)\sigma_{111}(x-z,y)\,dz = \quad \text{(B.2)}$$

$$
\begin{aligned}
&\frac{G}{2\pi(1-\nu_u)}\left[\frac{-1}{a}\int_{-2a_1}^{+2a_1}\left[\frac{8y(x-\mathfrak{z})^4}{((x-\mathfrak{z})^2+y^2)^3}-\frac{2y(x-\mathfrak{z})^2}{((x-\mathfrak{z})^2+y^2)^2}\right]d\mathfrak{z}+\frac{1}{2}\int_{-2a_1}^{+2a_1}\left[\frac{8y(x-\mathfrak{z})^3}{((x-\mathfrak{z})^2+y^2)^3}-\frac{2y(x-\mathfrak{z})}{((x-\mathfrak{z})^2+y^2)^2}\right]d\mathfrak{z}\right.\\
&\qquad+\frac{1}{a}\int_{-2a_2}^{+2a_2}\left[\frac{8y(x-\mathfrak{z})^4}{((x-\mathfrak{z})^2+y^2)^3}-\frac{2y(x-\mathfrak{z})^2}{((x-\mathfrak{z})^2+y^2)^2}\right]d\mathfrak{z}\Bigg]\\
&\qquad+\frac{1}{2}\int_{-2a_1}^{+2a_1}\left[\frac{8y(x-\mathfrak{z})^3}{((x-\mathfrak{z})^2+y^2)^3}-\frac{2y(x-\mathfrak{z})}{((x-\mathfrak{z})^2+y^2)^2}\right]d\mathfrak{z}=
\end{aligned}
$$

$$
\frac{G}{2\pi(1-\nu_u)}\left[\frac{1}{2}\left(\frac{y(3(x-\mathfrak{z})^2+y^2)}{((x-\mathfrak{z})^2+y^2)^2}\right)\Bigg|_{\mathfrak{z}=-2a_1}^{\mathfrak{z}=+2a_1}+\frac{1}{2}\left(\frac{y(3(x-\mathfrak{z})^2+y^2)}{((x-\mathfrak{z})^2+y^2)^2}\right)\Bigg|_{\mathfrak{z}=-2a_2}^{\mathfrak{z}=+2a_2}\right]=
$$

$$
\frac{G}{4\pi(1-\nu_u)}\left[\left(\frac{y(3(x-2a_1)^2+y^2)}{((x-2a_1)^2+y^2)^2}-\frac{y(3(x+2a_1)^2+y^2)}{((x+2a_1)^2+y^2)^2}\right)+\left(\frac{y(3(x-2a_2)^2+y^2)}{((x-2a_2)^2+y^2)^2}-\frac{y(3(x+2a_2)^2+y^2)}{((x+2a_2)^2+y^2)^2}\right)\right]
$$

$$
\sigma_{xx}^{dn,\lambda}=(D_n)_1\int_{-2a_1}^{+2a_1}N_1(x-\mathfrak{z})\sigma_{112}(x-\mathfrak{z},y)\,d\mathfrak{z}+(D_n)_2\int_{-2a_2}^{+2a_2}N_2(x-\mathfrak{z})\sigma_{112}(x-\mathfrak{z},y)\,d\mathfrak{z}=
$$

$$
\begin{aligned}
&\frac{G}{2\pi(1-\nu_u)}\left[\frac{-1}{a}\int_{-2a_1}^{+2a_1}\left[\frac{8(x-\mathfrak{z})^3y^2}{((x-\mathfrak{z})^2+y^2)^3}-\frac{(x-\mathfrak{z})}{((x-\mathfrak{z})^2+y^2)}\right]d\mathfrak{z}+\frac{1}{2}\int_{-2a_1}^{+2a_1}\left[\frac{8(x-\mathfrak{z})^2y^2}{((x-\mathfrak{z})^2+y^2)^3}-\frac{1}{((x-\mathfrak{z})^2+y^2)}\right]d\mathfrak{z}\right.\\
&\qquad+\frac{1}{a}\int_{-2a_2}^{+2a_2}\left[\frac{8(x-\mathfrak{z})^3y^2}{((x-\mathfrak{z})^2+y^2)^3}-\frac{(x-\mathfrak{z})}{((x-\mathfrak{z})^2+y^2)}\right]d\mathfrak{z}\\
&\qquad\left.+\frac{1}{2}\int_{-2a_2}^{+2a_2}\left[\frac{8(x-\mathfrak{z})^2y^2}{((x-\mathfrak{z})^2+y^2)^3}-\frac{1}{((x-\mathfrak{z})^2+y^2)}\right]d\mathfrak{z}\right]=
\end{aligned}
\tag{B.3}
$$

$$
\frac{G}{4\pi(1-\nu_u)}\left[\left(\frac{(x-\mathfrak{z})(y^2-(x-\mathfrak{z})^2)}{((x-\mathfrak{z})^2+y^2)^2}\right)\Bigg|_{\mathfrak{z}=-2a_1}^{\mathfrak{z}=+2a_1}+\left(\frac{(x-\mathfrak{z})(y^2-(x-\mathfrak{z})^2)}{((x-\mathfrak{z})^2+y^2)^2}\right)\Bigg|_{\mathfrak{z}=-2a_2}^{\mathfrak{z}=+2a_2}\right]=
$$

$$
\begin{aligned}
&\frac{G}{4\pi(1-\nu_u)}\left[\left(\frac{(x-2a_1)(y^2-(x-2a_1)^2)}{((x-2a_1)^2+y^2)^2}-\frac{(x+2a_1)(y^2-(x+2a_1)^2)}{((x+2a_1)^2+y^2)^2}\right)\right.\\
&\qquad\left.+\left(\frac{(x-2a_2)(y^2-(x-2a_2)^2)}{((x-2a_2)^2+y^2)^2}-\frac{(x+2a_2)(y^2-(x+2a_2)^2)}{((x+2a_2)^2+y^2)^2}\right)\right]
\end{aligned}
$$

$$
\begin{aligned}
&\sigma_{yy}^{dn,\lambda}=(D_n)_1\int_{-2a_1}^{+2a_1}N_1(x-\mathfrak{z})\sigma_{222}(x-\mathfrak{z},y)\,d\mathfrak{z}+(D_n)_2\int_{-2a_2}^{+2a_2}N_2(x-\mathfrak{z})\sigma_{222}(x-\mathfrak{z},y)\,d\mathfrak{z}\\
&\frac{G}{2\pi(1-\nu_u)}\left[\frac{-1}{a}\int_{-2a_1}^{+2a_1}\left[\frac{8(x-\mathfrak{z})y^4}{((x-\mathfrak{z})^2+y^2)^3}-\frac{4(x-\mathfrak{z})y^2}{((x-\mathfrak{z})^2+y^2)^2}-\frac{(x-\mathfrak{z})}{((x-\mathfrak{z})^2+y^2)}\right]d\mathfrak{z}\right.\\
&\qquad+\frac{1}{2}\int_{-2a_1}^{+2a_1}\left[\frac{8y^4}{((x-\mathfrak{z})^2+y^2)^3}-\frac{4y^2}{((x-\mathfrak{z})^2+y^2)^2}-\frac{1}{((x-\mathfrak{z})^2+y^2)}\right]d\mathfrak{z}\\
&\qquad+\frac{1}{a}\int_{-2a_2}^{+2a_2}\left[\frac{8(x-\mathfrak{z})y^4}{((x-\mathfrak{z})^2+y^2)^3}-\frac{4(x-\mathfrak{z})y^2}{((x-\mathfrak{z})^2+y^2)^2}-\frac{(x-\mathfrak{z})}{((x-\mathfrak{z})^2+y^2)}\right]d\mathfrak{z}\\
&\qquad\left.+\frac{1}{2}\int_{-2a_2}^{+2a_2}\left[\frac{8y^4}{((x-\mathfrak{z})^2+y^2)^3}-\frac{4y^2}{((x-\mathfrak{z})^2+y^2)^2}-\frac{1}{((x-\mathfrak{z})^2+y^2)}\right]d\mathfrak{z}\right]\\
&\qquad=-\frac{G}{4\pi(1-\nu_u)}\left[\left(\frac{(x-\mathfrak{z})((x-\mathfrak{z})^2+3y^2)}{((x-\mathfrak{z})^2+y^2)^2}\right)\Bigg|_{\mathfrak{z}=-2a_1}^{\mathfrak{z}=+2a_1}+\left(\frac{(x-\mathfrak{z})((x-\mathfrak{z})^2+3y^2)}{((x-\mathfrak{z})^2+y^2)^2}\right)\Bigg|_{\mathfrak{z}=-2a_2}^{\mathfrak{z}=+2a_2}\right]\\
&\qquad=-\frac{G}{4\pi(1-\nu_u)}\left[\left(\frac{(x-2a_1)((x-2a_1)^2+3y^2)}{((x-2a_1)^2+y^2)^2}-\frac{(x+2a_1)((x+2a_1)^2+3y^2)}{((x+2a_1)^2+y^2)^2}\right)\right.\\
&\qquad\left.+\left(\frac{(x-2a_2)((x-2a_2)^2+3y^2)}{((x-2a_2)^2+y^2)^2}-\frac{(x+2a_2)((x+2a_2)^2+3y^2)}{((x+2a_2)^2+y^2)^2}\right)\right]
\end{aligned}
\tag{B.4}
$$

$$\begin{aligned}\sigma_{yx}^{dn,\lambda} &= (D_n)_1 \int_{-2a_1}^{+2a_1} N_1(x-ʒ)\sigma_{212}(x-ʒ,y)\,dʒ + (D_n)_2 \int_{-2a_2}^{+2a_2} N_2(x-ʒ)\sigma_{212}(x-ʒ,y)\,dʒ = \frac{G}{2\pi(1-\nu_u)} \\ &= \frac{G}{4\pi(1-\nu_u)}\left[\left(\frac{y(y^2-(x-ʒ)^2)}{((x-ʒ)^2+y^2)^2}\right)\Bigg|_{ʒ=-2a_1}^{ʒ=+2a_1} + \left(\frac{y(y^2-(x-ʒ)^2)}{((x-ʒ)^2+y^2)^2}\right)\Bigg|_{ʒ=-2a_2}^{ʒ=+2a_2}\right] \\ &= \frac{G}{4\pi(1-\nu_u)}\left[\left(\frac{y(y^2-(x-2a_1)^2)}{((x-2a_1)^2+y^2)^2} - \frac{y(y^2-(x+2a_1)^2)}{((x+2a_1)^2+y^2)^2}\right)\right. \\ &\left.+\left(\frac{y(y^2-(x-2a_2)^2)}{((x-2a_2)^2+y^2)^2} - \frac{y(y^2-(x+2a_2)^2)}{((x+2a_2)^2+y^2)^2}\right)\right]\end{aligned} \tag{B.5}$$

$$\begin{aligned}P_x^{\lambda} &= (D_s)_1 \int_{-2a_1}^{+2a_1} N_1(x-ʒ)p_1(x-ʒ,y)dʒ + (D_s)_1 \int_{-2a_2}^{+2a_2} N_2(x-ʒ)p_1(x-ʒ,y)dʒ \\ &= -\frac{BG(1+\nu_u)}{3\pi(1-\nu_u)}\left[\frac{-1}{a}\int_{-2a_1}^{+2a_1}\left[\frac{2(x-ʒ)^2y}{((x-ʒ)^2+y^2)^2}\right]dʒ + \frac{1}{2}\int_{-2a_1}^{+2a_1}\left[\frac{2(x-ʒ)y}{((x-ʒ)^2+y^2)^2}\right]dʒ\right. \\ &\left.+\frac{1}{a}\int_{-2a_2}^{+2a_2}\left[\frac{2(x-ʒ)^2y}{((x-ʒ)^2+y^2)^2}\right]dʒ + \frac{1}{2}\int_{-2a_2}^{+2a_2}\left[\frac{2(x-ʒ)y}{((x-ʒ)^2+y^2)^2}\right]dʒ\right] \\ &= -\frac{SG(1+\nu_u)}{6\pi(1-\nu_u)}\left[\left(\frac{y}{(x-ʒ)^2+y^2}\right)\Bigg|_{ʒ=-2a_1}^{ʒ=+2a_1} + \left(\frac{y}{(x-ʒ)^2+y^2}\right)\Bigg|_{ʒ=-2a_2}^{ʒ=+2a_2}\right] \\ &= -\frac{SG(1+\nu_u)}{6\pi(1-\nu_u)}\left[\left(\frac{y}{(x-2a_1)^2+y^2} - \frac{y}{(x+2a_1)^2+y^2}\right) + \left(\frac{y}{(x-2a_2)^2+y^2} - \frac{y}{(x+2a_2)^2+y^2}\right)\right]\end{aligned} \tag{B.6}$$

Time-dependent part of influence functions

$$\begin{aligned}\odot\sigma_{yy}^{ds,\lambda} &= \frac{2Gc(\nu_u-\nu)}{\pi(1-\nu_u)(1-\nu)}\left[\frac{-1}{a}\frac{1}{((x-ʒ)^2+y^2)^3}\right. \\ &\times\left[y(3(x-ʒ)^3-y^2)\left[1-(1+\xi^2)e^{-\xi^2}\right]-2(x-ʒ)^3y\xi^4e^{-\xi^2}\right]\Big|_{ʒ=-2a_1}^{ʒ=+2a_1} + \frac{1}{2}\frac{1}{((x-ʒ)^2+y^2)^3} \\ &\times\left[y(3(x-ʒ)^2-y^2)\left[1-(1+\xi^2)e^{-\xi^2}\right]-2(x-ʒ)^2y\xi^4e^{-\xi^2}\right]\Big|_{ʒ=-2a_1}^{ʒ=+2a_1} + \frac{1}{a}\frac{1}{((x-ʒ)^2+y^2)^3} \\ &\times\left[y(3(x-ʒ)^3-y^2)\left[1-(1+\xi^2)e^{-\xi^2}\right]-2(x-ʒ)^3y\xi^4e^{-\xi^2}\right]\Big|_{ʒ=-2a_2}^{ʒ=+2a_2} + \frac{1}{2}\frac{1}{((x-ʒ)^2+y^2)^3} \\ &\left.\times\left[y(3(x-ʒ)^2-y^2)\left[1-(1+\xi^2)e^{-\xi^2}\right]-2(x-ʒ)^2y\xi^4e^{-\xi^2}\right]\Big|_{ʒ=-2a_2}^{ʒ=+2a_2}\right] \\ &= \frac{Gc(\nu_u-\nu)}{\pi(1-\nu_u)(1-\nu)}\left[\left(\frac{1}{((x-2a_1)^2+y^2)^3} - \frac{1}{((x+2a_1)^2+y^2)^3}\right)\right. \\ &\times\left[\left(y(3(x-2a_1)^2-y^2)\left[1-(1+\xi^2)e^{-\xi^2}\right]\right.\right. \\ &-2(x-2a_1)^2y\xi^4e^{-\xi^2}\Big)-\left(y(3(x+2a_1)^2-y^2)\left[1-(1+\xi^2)e^{-\xi^2}\right]-2(x+2a_1)^2y\xi^4e^{-\xi^2}\right)\Big] \\ &+\left(\frac{1}{((x-2a_2)^2+y^2)^3} - \frac{1}{((x+2a_2)^2+y^2)^3}\right) \\ &\times\left[\left(y(3(x-2a_2)^2-y^2)\left[1-(1+\xi^2)e^{-\xi^2}\right]\right.\right. \\ &\left.-2(x-2a_2)^2y\xi^4e^{-\xi^2}\Big)-\left(y(3(x+2a_2)^2-y^2)\left[1-(1+\xi^2)e^{-\xi^2}\right]-2(x+2a_2)^2y\xi^4e^{-\xi^2}\right)\Big]\right]\end{aligned} \tag{B.7}$$

$$
\begin{aligned}
\odot\sigma_{xx}^{ds,\lambda} &= \frac{2Gc(\nu_u-\nu)}{\pi(1-\nu_u)(1-\nu)}\Big[\frac{-1}{a}\frac{1}{((x-\mathfrak{z})^2+y^2)^3}\times\left(y(y^2-3(x-\mathfrak{z})^3)\left[1-(1+\xi^2)e^{-\xi^2}\right]-2y^3\xi^4e^{-\xi^2}\right)\Big|_{\mathfrak{z}=-2a_1}^{\mathfrak{z}=+2a_1} \\
&+\frac{1}{2}\frac{1}{((x-\mathfrak{z})^2+y^2)^3}\times\left(y(y^2-3(x-\mathfrak{z})^2)\left[1-(1+\xi^2)e^{-\xi^2}\right]-2y^3\xi^4e^{-\xi^2}\right)\Big|_{\mathfrak{z}=-2a_1}^{\mathfrak{z}=+2a_1} \\
&+\frac{1}{a}\frac{1}{((x-\mathfrak{z})^2+y^2)^3}\left(y(y^2-3(x-\mathfrak{z})^3)\left[1-(1+\xi^2)e^{-\xi^2}\right]-2y^3\xi^4e^{-\xi^2}\right)\Big|_{\mathfrak{z}=-2a_2}^{\mathfrak{z}=+2a_2} \\
&+\frac{1}{2}\frac{1}{((x-\mathfrak{z})^2+y^2)^3}\left(y(y^2-3(x-\mathfrak{z})^2)\left[1-(1+\xi^2)e^{-\xi^2}\right]-2y^3\xi^4e^{-\xi^2}\right)\Big|_{\mathfrak{z}=-2a_2}^{\mathfrak{z}=+2a_2}\Big] \\
&= \frac{Gc(\nu_u-\nu)}{\pi(1-\nu_u)(1-\nu)}\Big\{\left[1-(1+\xi^2)e^{-\xi^2}-2y^3\xi^4e^{-\xi^2}\right]\frac{y(y^2-3(x-2a_1)^2)}{((x-2a_1)^2+y^2)^3} \\
&-\frac{y(y^2-3(x+2a_1)^2)}{((x+2a_1)^2+y^2)^3}-\frac{2y^3\xi^4e^{-\xi^2}}{((x-2a_1)^2+y^2)^3}+\frac{2y^3\xi^4e^{-\xi^2}}{((x+2a_1)^2+y^2)^3} \\
&+\left[1-(1+\xi^2)e^{-\xi^2}-2y^3\xi^4e^{-\xi^2}\right]\frac{y(y^2-3(x-2a_2)^2)}{((x-2a_2)^2+y^2)^3}-\frac{y(y^2-3(x+2a_2)^2)}{((x+2a_2)^2+y^2)^3} \\
&-\frac{2y^3\xi^4e^{-\xi^2}}{((x-2a_2)^2+y^2)^3}+\frac{2y^3\xi^4e^{-\xi^2}}{((x+2a_2)^2+y^2)^3}\Big\}
\end{aligned}
\tag{B.8}
$$

$$
\begin{aligned}
\odot\sigma_{xx}^{ds,\lambda} &= \frac{2Gc(\nu_u-\nu)}{\pi(1-\nu_u)(1-\nu)}\Big[\frac{-1}{a}\frac{1}{((x-\mathfrak{z})^2+y^2)^3}\times\left(y(y^2-3(x-\mathfrak{z})^3)\left[1-(1+\xi^2)e^{-\xi^2}\right]-2y^3\xi^4e^{-\xi^2}\right)\Big|_{\mathfrak{z}=-2a_1}^{\mathfrak{z}=+2a_1} \\
&+\frac{1}{2}\frac{1}{((x-\mathfrak{z})^2+y^2)^3}\times\left(y(y^2-3(x-\mathfrak{z})^2)\left[1-(1+\xi^2)e^{-\xi^2}\right]-2y^3\xi^4e^{-\xi^2}\right)\Big|_{\mathfrak{z}=-2a_1}^{\mathfrak{z}=+2a_1} \\
&+\frac{1}{a}\frac{1}{((x-\mathfrak{z})^2+y^2)^3}\left(y(y^2-3(x-\mathfrak{z})^3)\left[1-(1+\xi^2)e^{-\xi^2}\right]-2y^3\xi^4e^{-\xi^2}\right)\Big|_{\mathfrak{z}=-2a_2}^{\mathfrak{z}=+2a_2} \\
&+\frac{1}{2}\frac{1}{((x-\mathfrak{z})^2+y^2)^3}\left(y(y^2-3(x-\mathfrak{z})^2)\left[1-(1+\xi^2)e^{-\xi^2}\right]-2y^3\xi^4e^{-\xi^2}\right)\Big|_{\mathfrak{z}=-2a_2}^{\mathfrak{z}=+2a_2}\Big] \\
&= \frac{Gc(\nu_u-\nu)}{\pi(1-\nu_u)(1-\nu)}\Big\{\left[1-(1+\xi^2)e^{-\xi^2}-2y^3\xi^4e^{-\xi^2}\right]\frac{y(y^2-3(x-2a_1)^2)}{((x-2a_1)^2+y^2)^3} \\
&-\frac{y(y^2-3(x+2a_1)^2)}{((x+2a_1)^2+y^2)^3}-\frac{2y^3\xi^4e^{-\xi^2}}{((x-2a_1)^2+y^2)^3}+\frac{2y^3\xi^4e^{-\xi^2}}{((x+2a_1)^2+y^2)^3} \\
&+\left[1-(1+\xi^2)e^{-\xi^2}-2y^3\xi^4e^{-\xi^2}\right]\frac{y(y^2-3(x-2a_2)^2)}{((x-2a_2)^2+y^2)^3}-\frac{y(y^2-3(x+2a_2)^2)}{((x+2a_2)^2+y^2)^3} \\
&-\frac{2y^3\xi^4e^{-\xi^2}}{((x-2a_2)^2+y^2)^3}+\frac{2y^3\xi^4e^{-\xi^2}}{((x+2a_2)^2+y^2)^3}\Big\}
\end{aligned}
\tag{B.9}
$$

$$
\begin{aligned}
\odot\sigma_{xx}^{dn,\lambda} &= \frac{2Gc(\nu_u-\nu)}{\pi(1-\nu_u)(1-\nu)}\Big[\frac{-1}{a}\frac{1}{((x-\mathfrak{z})^2+y^2)^3} \\
&\times\left[(x-\mathfrak{z})^2((x-\mathfrak{z})^3-3y^2)\left[1-(1+\xi^2)e^{-\xi^2}\right]+2(x-\mathfrak{z})^2y^2\xi^4e^{-\xi^2}\right]\Big|_{\mathfrak{z}=-2a_1}^{\mathfrak{z}=+2a_1} \\
&+\frac{1}{2}\frac{1}{((x-\mathfrak{z})^2+y^2)^3} \\
&\times\left[(x-\mathfrak{z})((x-\mathfrak{z})^2-3y^2)\left[1-(1+\xi^2)e^{-\xi^2}\right]+2(x-\mathfrak{z})y^2\xi^4e^{-\xi^2}\right]\Big|_{\mathfrak{z}=-2a_1}^{\mathfrak{z}=+2a_1} \\
&+\frac{1}{a}\frac{1}{((x-\mathfrak{z})^2+y^2)^3} \\
&\times\left[(x-\mathfrak{z})^2((x-\mathfrak{z})^3-3y^2)\left[1-(1+\xi^2)e^{-\xi^2}\right]+2(x-\mathfrak{z})^2y^2\xi^4e^{-\xi^2}\right]\Big|_{\mathfrak{z}=-2a_2}^{\mathfrak{z}=+2a_2} \\
&+\frac{1}{2}\frac{1}{((x-\mathfrak{z})^2+y^2)^3} \\
&\times\left[(x-\mathfrak{z})((x-\mathfrak{z})^2-3y^2)\left[1-(1+\xi^2)e^{-\xi^2}\right]+2(x-\mathfrak{z})y^2\xi^4e^{-\xi^2}\right]\Big|_{\mathfrak{z}=-2a_2}^{\mathfrak{z}=+2a_2}\Big] \\
&= \frac{Gc(\nu_u-\nu)}{\pi(1-\nu_u)(1-\nu)}\Big[\Big(\frac{1}{((x-2a_1)^2+y^2)^3}-\frac{1}{((x+2a_1)^2+y^2)^3}\Big) \\
&\times\left(\left[(x-2a_1)((x-2a_1)^2-3y^2)\left[1-(1+\xi^2)e^{-\xi^2}\right]+2(x-2a_1)y^2\xi^4e^{-\xi^2}\right)\right. \\
&-\Big((x+2a_1)((x+2a_1)^2-3y^2)\left[1-(1+\xi^2)e^{-\xi^2}\right]\Big)+2(x+2a_1)y^2\xi^4e^{-\xi^2}\Big) \\
&+\Big(\frac{1}{((x-2a_2)^2+y^2)^3}-\frac{1}{((x+2a_2)^2+y^2)^3}\Big) \\
&\times\left(\left[(x-2a_2)((x-2a_2)^2-3y^2)\left[1-(1+\xi^2)e^{-\xi^2}\right]+2(x-2a_2)y^2\xi^4e^{-\xi^2}\right)\right. \\
&-\Big((x+2a_2)((x+2a_2)^2-3y^2)\left[1-(1+\xi^2)e^{-\xi^2}\right]\Big)+2(x+2a_2)y^2\xi^4e^{-\xi^2}\Big)\Big]
\end{aligned}
\tag{B.10}
$$

$$
\begin{aligned}
\odot\sigma_{yy}^{dn,\lambda} &= \frac{2Gc(\nu_u-\nu)}{\pi(1-\nu_u)(1-\nu)}\Bigg[\frac{-1}{a}\frac{1}{((x-\mathfrak{z})^2+y^2)^3} \\
&\times\left[(x-\mathfrak{z})^2(3y^2-(x-\mathfrak{z})^3)\left[1-(1+\xi^2)e^{-\xi^2}\right]+2(x-\mathfrak{z})^4\xi^4e^{-\xi^2}\right]\Big|_{\mathfrak{z}=-2a_1}^{\mathfrak{z}=+2a_1} \\
&+\frac{1}{2}\frac{1}{((x-\mathfrak{z})^2+y^2)^3}\times\left[(x-\mathfrak{z})(3y^2-(x-\mathfrak{z})^2)\left[1-(1+\xi^2)e^{-\xi^2}\right]+2(x-\mathfrak{z})^3\xi^4e^{-\xi^2}\right]\Big|_{\mathfrak{z}=-2a_1}^{\mathfrak{z}=+2a_1} \\
&+\frac{1}{a}\frac{1}{((x-\mathfrak{z})^2+y^2)^3} \\
&\times\left[(x-\mathfrak{z})^2(3y^2-(x-\mathfrak{z})^3)\left[1-(1+\xi^2)e^{-\xi^2}\right]+2(x-\mathfrak{z})^4\xi^4e^{-\xi^2}\right]\Big|_{\mathfrak{z}=-2a_2}^{\mathfrak{z}=+2a_2} \\
&+\frac{1}{2}\frac{1}{((x-\mathfrak{z})^2+y^2)^3} \\
&\times\left[(x-\mathfrak{z})(3y^2-(x-\mathfrak{z})^2)\left[1-(1+\xi^2)e^{-\xi^2}\right]+2(x-\mathfrak{z})^3\xi^4e^{-\xi^2}\right]\Big|_{\mathfrak{z}=-2a_2}^{\mathfrak{z}=+2a_2}\Bigg] \\
&= \frac{Gc(\nu_u-\nu)}{\pi(1-\nu_u)(1-\nu)}\Bigg[\left(\frac{1}{((x-2a_1)^2+y^2)^3}-\frac{1}{((x+2a_1)^2+y^2)^3}\right) \\
&\times\Big(\Big[(x-2a_1)(3y^2-(x-2a_1)^2)\left[1-(1+\xi^2)e^{-\xi^2}\right]+2(x-2a_1)^3\xi^4e^{-\xi^2}\Big] \\
&-\left[(x+2a_1)(3y^2-(x+2a_1)^2)\left[1-(1+\xi^2)e^{-\xi^2}\right]+2(x+2a_1)^3\xi^4e^{-\xi^2}\right]\Big) \\
&+\left(\frac{1}{((x-2a_2)^2+y^2)^3}-\frac{1}{((x+2a_2)^2+y^2)^3}\right) \\
&\times\Big(\left[(x-2a_2)(3y^2-(x-2a_2)^2)\left[1-(1+\xi^2)e^{-\xi^2}\right]+2(x-2a_2)^3\xi^4e^{-\xi^2}\right] \\
&-\left[(x+2a_2)(3y^2-(x+2a_2)^2)\left[1-(1+\xi^2)e^{-\xi^2}\right]+2(x+2a_2)^3\xi^4e^{-\xi^2}\right]\Big)\Bigg]
\end{aligned}
\tag{B.11}
$$

$$
\begin{aligned}
\odot\sigma_{yx}^{dn,\lambda} &= \frac{2Gc(\nu_u-\nu)}{\pi(1-\nu_u)(1-\nu)}\Bigg[\frac{-1}{a}\frac{1}{((x-\mathfrak{z})^2+y^2)^3} \\
&\times\left[y(3(x-\mathfrak{z})^3-y^2)\left[1-(1+\xi^2)e^{-\xi^2}\right]-2(x-\mathfrak{z})^3y\xi^4e^{-\xi^2}\right]\Big|_{\mathfrak{z}=-2a_1}^{\mathfrak{z}=+2a_1}+\frac{1}{2}\frac{1}{((x-\mathfrak{z})^2+y^2)^3} \\
&\times\left[y(3(x-\mathfrak{z})^2-y^2)\left[1-(1+\xi^2)e^{-\xi^2}\right]-2(x-\mathfrak{z})^2y\xi^4e^{-\xi^2}\right]\Big|_{\mathfrak{z}=-2a_1}^{\mathfrak{z}=+2a_1}+\frac{1}{a}\frac{1}{((x-\mathfrak{z})^2+y^2)^3} \\
&\times\left[y(3(x-\mathfrak{z})^3-y^2)\left[1-(1+\xi^2)e^{-\xi^2}\right]-2(x-\mathfrak{z})^3y\xi^4e^{-\xi^2}\right]\Big|_{\mathfrak{z}=-2a_2}^{\mathfrak{z}=+2a_2}+\frac{1}{2}\frac{1}{((x-\mathfrak{z})^2+y^2)^3} \\
&\times\left[y(3(x-\mathfrak{z})^2-y^2)\left[1-(1+\xi^2)e^{-\xi^2}\right]-2(x-\mathfrak{z})^2y\xi^4e^{-\xi^2}\right]\Big|_{\mathfrak{z}=-2a_2}^{\mathfrak{z}=+2a_2}\Bigg] \\
&= \frac{Gc(\nu_u-\nu)}{\pi(1-\nu_u)(1-\nu)}\Bigg[\left(\frac{1}{((x-2a_1)^2+y^2)^3}-\frac{1}{((x+2a_1)^2+y^2)^3}\right) \\
&\times\Big[\Big(y(3(x-2a_1)^2-y^2)\left[1-(1+\xi^2)e^{-\xi^2}\right] \\
&-2(x-2a_1)^2y\xi^4e^{-\xi^2}\Big)-\Big(y(3(x+2a_1)^2-y^2)\left[1-(1+\xi^2)e^{-\xi^2}\right]-2(x+2a_1)^2y\xi^4e^{-\xi^2}\Big)\Big] \\
&+\left(\frac{1}{((x-2a_2)^2+y^2)^3}-\frac{1}{((x+2a_2)^2+y^2)^3}\right) \\
&\times\Big[\Big(y(3(x-2a_2)^2-y^2)\left[1-(1+\xi^2)e^{-\xi^2}\right] \\
&-2(x-2a_2)^2y\xi^4e^{-\xi^2}\Big)-\Big(y(3(x+2a_2)^2-y^2)\left[1-(1+\xi^2)e^{-\xi^2}\right]-2(x+2a_2)^2y\xi^4e^{-\xi^2}\Big)\Big]\Bigg]
\end{aligned}
\tag{B.11}
$$

$$
\begin{aligned}
\odot\sigma_{yx}^{dn,\lambda} &= \frac{2Gc(\nu_u-\nu)}{\pi(1-\nu_u)(1-\nu)}\Bigg[\frac{-1}{a}\frac{1}{((x-\mathfrak{z})^2+y^2)^3} \\
&\times \left[y(3(x-\mathfrak{z})^3-y^2)\left[1-(1+\xi^2)e^{-\xi^2}\right]-2(x-\mathfrak{z})^3y\xi^4e^{-\xi^2}\right]\Big|_{\mathfrak{z}=-2a_1}^{\mathfrak{z}=+2a_1}+\frac{1}{2}\frac{1}{((x-\mathfrak{z})^2+y^2)^3} \\
&\times \left[y(3(x-\mathfrak{z})^2-y^2)\left[1-(1+\xi^2)e^{-\xi^2}\right]-2(x-\mathfrak{z})^2y\xi^4e^{-\xi^2}\right]\Big|_{\mathfrak{z}=-2a_1}^{\mathfrak{z}=+2a_1}+\frac{1}{a}\frac{1}{((x-\mathfrak{z})^2+y^2)^3} \\
&\times \left[y(3(x-\mathfrak{z})^3-y^2)\left[1-(1+\xi^2)e^{-\xi^2}\right]-2(x-\mathfrak{z})^3y\xi^4e^{-\xi^2}\right]\Big|_{\mathfrak{z}=-2a_2}^{\mathfrak{z}=+2a_2}+\frac{1}{2}\frac{1}{((x-\mathfrak{z})^2+y^2)^3} \\
&\times \left[y(3(x-\mathfrak{z})^2-y^2)\left[1-(1+\xi^2)e^{-\xi^2}\right]-2(x-\mathfrak{z})^2y\xi^4e^{-\xi^2}\right]\Big|_{\mathfrak{z}=-2a_2}^{\mathfrak{z}=+2a_2}\Bigg] \\
&= \frac{Gc(\nu_u-\nu)}{\pi(1-\nu_u)(1-\nu)}\Bigg[\left(\frac{1}{((x-2a_1)^2+y^2)^3}-\frac{1}{((x+2a_1)^2+y^2)^3}\right) \\
&\times \Big[\Big(y(3(x-2a_1)^2-y^2)\left[1-(1+\xi^2)e^{-\xi^2}\right] \\
&-2(x-2a_1)^2y\xi^4e^{-\xi^2}\Big)-\Big(y(3(x+2a_1)^2-y^2)\left[1-(1+\xi^2)e^{-\xi^2}\right]-2(x+2a_1)^2y\xi^4e^{-\xi^2}\Big)\Big] \\
&+\left(\frac{1}{((x-2a_2)^2+y^2)^3}-\frac{1}{((x+2a_2)^2+y^2)^3}\right) \\
&\times \Big[\Big(y(3(x-2a_2)^2-y^2)\left[1-(1+\xi^2)e^{-\xi^2}\right] \\
&-2(x-2a_2)^2y\xi^4e^{-\xi^2}\Big)-\Big(y(3(x+2a_2)^2-y^2)\left[1-(1+\xi^2)e^{-\xi^2}\right]-2(x+2a_2)^2y\xi^4e^{-\xi^2}\Big)\Big]\Bigg]
\end{aligned}
\tag{B.12}
$$

$$
\begin{aligned}
\odot\sigma_{xx}^{df,\lambda} &= \frac{SG(1+\nu_u)}{6\pi(1-\nu_u)}\Bigg[\Bigg[\sqrt{\frac{\pi}{((x-\mathfrak{z})^2+y^2)}}\,\xi erf\left(\frac{(x-\mathfrak{z})\xi}{(x-\mathfrak{z})^2+y^2}\right)e^{(-(y^2/(x-\mathfrak{z})^2+y^2)\xi^2)} \\
&-\frac{(x-\mathfrak{z})}{(x-\mathfrak{z})^2+y^2}\left(1-e^{-\xi^2}\right)\Bigg]\Bigg|_{\mathfrak{z}=-2a_1}^{\mathfrak{z}=+2a_1} \\
&+\Bigg[\sqrt{\frac{\pi}{((x-\mathfrak{z})^2+y^2)}}\,\xi erf\left(\frac{(x-\mathfrak{z})\xi}{(x-\mathfrak{z})^2+y^2}\right)e^{(-(y^2/(x-\mathfrak{z})^2+y^2)\xi^2)} \\
&-\frac{(x-\mathfrak{z})}{(x-\mathfrak{z})^2+y^2}\left(1-e^{-\xi^2}\right)\Bigg]\Bigg|_{\mathfrak{z}=-2a_2}^{\mathfrak{z}=+2a_2}\Bigg] \\
&= \frac{SG(1+\nu_u)}{6\pi(1-\nu_u)}\Bigg\{\Bigg[\Bigg[\sqrt{\frac{\pi}{((x-2a_1)^2+y^2)}}\,\xi erf\left(\frac{(x-2a_1)\xi}{(x-2a_1)^2+y^2}\right)e^{(-(y^2/(x-2a_1)^2+y^2)\xi^2)} \\
&-\frac{(x-2a_1)}{(x-2a_1)^2+y^2}\left(1-e^{-\xi^2}\right) \\
&-\Bigg[\sqrt{\frac{\pi}{((x+2a_1)^2+y^2)}}\,\xi erf\left(\frac{(x+2a_1)\xi}{(x+2a_1)^2+y^2}\right)e^{(-(y^2/(x+2a_1)^2+y^2)\xi^2)} \\
&-\frac{(x+2a_1)}{(x+2a_1)^2+y^2}\left(1-e^{-\xi^2}\right)\Bigg]\Bigg] \\
&+\Bigg[\sqrt{\frac{\pi}{((x-2a_2)^2+y^2)}}\,\xi erf\left(\frac{(x-2a_2)\xi}{(x-2a_2)^2+y^2}\right)e^{(-(y^2/(x-2a_2)^2+y^2)\xi^2)} \\
&-\frac{(x-2a_2)}{(x-2a_2)^2+y^2}\left(1-e^{-\xi^2}\right) \\
&-\Bigg[\sqrt{\frac{\pi}{((x+2a_2)^2+y^2)}}\,\xi erf\left(\frac{(x+2a_2)\xi}{(x+2a_2)^2+y^2}\right)e^{(-(y^2/(x+2a_2)^2+y^2)\xi^2)} \\
&-\frac{(x+2a_2)}{(x+2a_2)^2+y^2}\left(1-e^{-\xi^2}\right)\Bigg]\Bigg]\Bigg\}
\end{aligned}
\tag{B.13}
$$

$$\odot\sigma_{yy}^{df,\lambda}=\frac{SG(1+\nu_u)}{6\pi(1-\nu_u)}\left[\left[\frac{(x-\mathfrak{z})}{(x-\mathfrak{z})^2+y^2}\left(1-e^{-\xi^2}\right)\right]\Bigg|_{\mathfrak{z}=-2a_1}^{\mathfrak{z}=+2a_2}+\left[\frac{(x-\mathfrak{z})}{(x-\mathfrak{z})^2+y^2}\left(1-e^{-\xi^2}\right)\right]\Bigg|_{\mathfrak{z}=-2a_2}^{\mathfrak{z}=+2a_2}\right]$$
$$=\frac{SG(1+\nu_u)}{6\pi(1-\nu_u)}\left(1-e^{-\xi^2}\right)\left[\left[\frac{(x-2a_2)}{(x-2a_2)^2+y^2}-\frac{(x+2a_1)}{(x+2a_1)^2+y^2}\right]+\left[\frac{(x-2a_2)}{(x-2a_2)^2+y^2}-\frac{(x+2a_2)}{(x+2a_2)^2+y^2}\right]\right] \quad \text{(B.14)}$$

$$\odot\sigma_{yx}^{df,\lambda}=-\frac{SG(1+\nu_u)}{6\pi(1-\nu_u)}\left[\left[\frac{y}{(x-\mathfrak{z})^2+y^2}\left(1-e^{-\xi^2}\right)\right]\Bigg|_{\mathfrak{z}=-2a_1}^{\mathfrak{z}=+2a_1}+\left[\frac{y}{(x-\mathfrak{z})^2+y^2}\left(1-e^{-\xi^2}\right)\right]\Bigg|_{\mathfrak{z}=-2a_2}^{\mathfrak{z}=+2a_2}\right]$$
$$=-\frac{SG(1+\nu_u)}{6\pi(1-\nu_u)}\left(1-e^{-\xi^2}\right)\left[\left[\frac{y}{(x-2a_1)^2+y^2}-\frac{y}{(x+2a_1)^2+y^2}\right]+\left[\frac{y}{(x-2a_2)^2+y^2}-\frac{y}{(x+2a_2)^2+y^2}\right]\right] \quad \text{(B.15)}$$

$$\odot P_x^{\lambda}=-\frac{4SGc(1+\nu_u)}{3\pi(1-\nu_u)}\left[\frac{-1}{a}\left[\frac{(x-\mathfrak{z})y}{((x-\mathfrak{z})^2+y^2)^2}\xi^4e^{-\xi^2}\right]\Bigg|_{\mathfrak{z}=-2a_1}^{\mathfrak{z}=+2a_1}+\frac{1}{2}\left[\frac{y}{((x-\mathfrak{z})^2+y^2)^2}\xi^4e^{-\xi^2}\right]\Bigg|_{\mathfrak{z}=-2a_1}^{\mathfrak{z}=+2a_1}\right.$$
$$\left.+\frac{1}{a}\left[\frac{(x-\mathfrak{z})y}{((x-\mathfrak{z})^2+y^2)^2}\xi^4e^{-\xi^2}\right]\Bigg|_{\mathfrak{z}=-2a_2}^{\mathfrak{z}=+2a_2}+\frac{1}{2}\left[\frac{y}{((x-\mathfrak{z})^2+y^2)^2}\xi^4e^{-\xi^2}\right]\Bigg|_{\mathfrak{z}=-2a_2}^{\mathfrak{z}=+2a_2}\right]$$
$$=-\frac{2SGc(1+\nu_u)}{3\pi(1-\nu_u)}\xi^4e^{-\xi^2}\left[\left[\frac{y}{((x-2a_1)^2+y^2)^2}-\frac{y}{((x+2a_1)^2+y^2)^2}\right]+\left[\frac{y}{((x-2a_2)^2+y^2)^2}-\frac{y}{((x+2a_2)^2+y^2)^2}\right]\right] \quad \text{(B.16)}$$

$$\odot P_y^{\lambda}=-\frac{4SGc(1+\nu_u)}{3\pi(1-\nu_u)}\left[\frac{-1}{a}\left[\frac{(x-\mathfrak{z})^2}{((x-\mathfrak{z})^2+y^2)^2}\xi^4e^{-\xi^2}\right]\Bigg|_{\mathfrak{z}=-2a_1}^{\mathfrak{z}=+2a_1}+\frac{1}{2}\left[\frac{(x-\mathfrak{z})}{((x-\mathfrak{z})^2+y^2)^2}\xi^4e^{-\xi^2}\right]\Bigg|_{\mathfrak{z}=-2a_1}^{\mathfrak{z}=+2a_1}\right.$$
$$\left.+\frac{-1}{a}\left[\frac{(x-\mathfrak{z})^2}{((x-\mathfrak{z})^2+y^2)^2}\xi^4e^{-\xi^2}\right]\Bigg|_{\mathfrak{z}=-2a_2}^{\mathfrak{z}=+2a_2}+\frac{1}{2}\left[\frac{(x-\mathfrak{z})}{((x-\mathfrak{z})^2+y^2)^2}\xi^4e^{-\xi^2}\right]\Bigg|_{\mathfrak{z}=-2a_2}^{\mathfrak{z}=+2a_2}\right]$$
$$=-\frac{2SGc(1+\nu_u)}{3\pi(1-\nu_u)}\xi^4e^{-\xi^2}\left[\left[\frac{(x-2a_1)}{((x-2a_1)^2+y^2)^2}-\frac{(x+2a_1)}{((x+2a_1)^2+y^2)^2}\right]+\left[\frac{(x-2a_2)}{((x-2a_2)^2+y^2)^2}-\frac{(x+2a_2)}{((x+2a_2)^2+y^2)^2}\right]\right] \quad \text{(B.17)}$$

$$
\begin{aligned}
&\odot P_f^{\lambda} \\
&= \frac{S^2 G(1-\nu)(1+\nu_u)^2}{9\pi(1-\nu_u)(\nu_u-\nu)}\Bigg\{\Bigg(\Bigg[\sqrt{\frac{\pi}{2((x-\mathfrak{z})^2+y^2)}}\xi erf\left(\frac{(x-\mathfrak{z})\xi}{(x-\mathfrak{z})^2+y^2}\right)e^{(-(y^2/(x-\mathfrak{z})^2+y^2)\xi^2)}\Bigg]\Bigg|_{\mathfrak{z}=-2a_1}^{\mathfrak{z}=+2a_1} \\
&+\Bigg[\sqrt{\frac{\pi}{2((x-\mathfrak{z})^2+y^2)}}\xi erf\left(\frac{(x-\mathfrak{z})\xi}{(x-\mathfrak{z})^2+y^2}\right)e^{(-(y^2/(x-\mathfrak{z})^2+y^2)\xi^2)}\Bigg]\Bigg|_{\mathfrak{z}=-2a_2}^{\mathfrak{z}=+2a_2}\Bigg\} \\
&= \frac{S^2 G(1-\nu)(1+\nu_u)^2}{9\pi(1-\nu_u)(\nu_u-\nu)}\Bigg\{\Bigg(\Bigg[\Bigg[\sqrt{\frac{\pi}{2((x-2a_1)^2+y^2)}}\xi erf\left(\frac{(x-2a_1)\xi}{(x-2a_1)^2+y^2}\right)e^{(-(y^2/(x-2a_1)^2+y^2)\xi^2)}\Bigg] \\
&-\Bigg[\sqrt{\frac{\pi}{2((x+2a_1)^2+y^2)}}\xi erf\left(\frac{(x+2a_1)\xi}{(x+2a_1)^2+y^2}\right)e^{(-(y^2/(x+2a_1)^2+y^2)\xi^2)}\Bigg]\Bigg] \\
&+\Bigg[\Bigg[\sqrt{\frac{\pi}{2((x-2a_2)^2+y^2)}}\xi erf\left(\frac{(x-2a)\xi}{(x-2a_2)^2+y^2}\right)e^{(-(y^2/(x-2a_2)^2+y^2)\xi^2)}\Bigg] \\
&-\Bigg[\sqrt{\frac{\pi}{2((x+2a_2)^2+y^2)}}\xi erf\left(\frac{(x+2a_2)\xi}{(x+2a_2)^2+y^2}\right)e^{(-(y^2/(x+2a_2)^2+y^2)\xi^2)}\Bigg]\Bigg]\Bigg)\Bigg\}
\end{aligned}
\qquad \text{(sB.18)}
$$

حل تحلیلی المان‌های ناپیوستگی جابجایی مرتبه اول در پوروالاستیسیته

محمد حسین دهقانی فیروزآبادی[1]، محمد فاتحی مرجی[1]، ابوالفضل عبدالهی پور[2*]، علیرضا یار احمدی بافقی[1] و یوسف میرزائیان[1]

1-دانشکده مهندسی معدن و متالورژی، دانشگاه یزد، یزد،ایران

2-دانشکده مهندسی معدن، دانشگاه تهران، تهران، ایران

ارسال 2023/02/07، پذیرش 2023/05/16

* نویسنده مسئول مکاتبات: Abdollahipour@ut.ac.ir

چکیده:

وجود منافذ و ترک‌ها در سنگ‌های متخلخل و شکسته شده اغلب با جریال سیال همراه است. پوروالاستیسیته می‌تواند برای مدل‌سازی دقیق بسیاری از ساختارهای سنگی در صنعت نفت استفاده شود. نزدیک شدن تنش به مقدار تنش شکست و اثر فشارمنفذی روی تغییر شکل سنگ، از جمله اثرات سیال روی رفتار مکانیکی محیط است. به دلیل ویژگی تغییر شکل- نفوذ محیط پوروالاستیک، معادلات حاکم، روابط جابجایی-کرنش و تنش-کرنش می‌توانند به یکدیگر تغییر کنند. در این مطالعه، معادلات اساسی و روابطی که برای بررسی رفتار و واکنش سنگ در یک محیط متخلخل لازم است بیان شده است. معادلات دیفرانسیلی مستقل و وابسته به زمان برای یک تکانه و منبع سیال نقطه ای به منظور به‌دست آوردن حل‌های اساسی استفاده می‌شود. توابع تاثیر با مشارکت دادن توابع شکل در فرمولاسیون حل‌های اساسی و انتگرال گیری از آنها حاصل می‌شود. برای کنترل اعتبار و درستی فرمولاسیون تهیه شده چند مثال ذکر شده است. در دو مثال اول، از برنامه کاربردی عددی و حل تحلیلی در زمان‌های مختلف و در شرایط زهکشی نشده و زهکشی شده استفاده شده است. در زمان‌های صفر(واکنش زهکشی نشده محیط) و 4500 ثانیه (واکنش زهکشی شده محیط)، بین نتایج عددی و تحلیلی هماهنگی و توافق خوبی وجود دارد. در مثال سوم، با استفاده از برنامه کاربردی عددی، مسیر انتشار ترک در دیواره چاه بدست آمده است که با نتایج طبیعی سازگاری دارد.

کلمات کلیدی: روش ناپیوستگی جابجایی، المان‌های مرتبه اول، پوروالاستیک،فشار منفذی، حل‌های اساسی، توابع تاثیر